minerals

MDPI

Article

Thermal Maturity and Kerogen Type of Badenian Dispersed Organic Matter from the Getic Depression, Romania

Maria Doina Ghiran [1,2], Mihai Emilian Popa [2,3,4,*], Izabela Mariş [5], Georgeta Predeanu [6], Ştefania Gheorghe [1] and Niculina Mihaela Bălănescu [6]

1 OMV PETROM S.A.-I.C.P.T. Câmpina, 29 Culturii Ave., 105600 Câmpina, Romania
2 Doctoral School, Faculty of Geology and Geophysics, University of Bucharest, 6 Traian Vuia Str., 020956 Bucharest, Romania
3 Laboratory of Palaeontology, Department of Geology, Faculty of Geology and Geophysics, University of Bucharest, 1 N. Bălcescu Ave., 011401 Bucharest, Romania
4 School of Geosciences and Technology, Southwest Petroleum University, 8, Xindu Ave., Chengdu 610500, China
5 Department of Mineralogy, Faculty of Geology and Geophysics, University of Bucharest, 1 N. Bălcescu Ave., 011401 Bucharest, Romania
6 Research Center for Environmental Protection and Ecofriendly Technologies, University Politehnica of Bucharest, 1-7 Gheorghe Polizu Str., 011061 Bucharest, Romania
* Correspondence: mihai@mepopa.com

Abstract: The aim of this study is to evaluate the thermal maturity of Upper Badenian (Middle Miocene) petroleum source rocks of the Getic Depression, Romania, and to characterize the dispersed organic matter using organic petrography associated with Rock-Eval pyrolysis. A total of 33 core samples of Upper Badenian source rocks from the central–southern part of Getic Depression was studied. The results show that most samples with values of total organic carbon (TOC) < 1% wt.% have a limited potential of hydrocarbons (HC) generation, and 30% of samples with TOC < 1.82 wt.% and kerogen type III, presenting particularly gas generation potential. In three samples from the Bibeşti, Grădişte and Socu structures the kerogen type III-II was identified, indicating the capability of oil and gas generation. The Badenian source rocks are thermally immature, as few samples are in the pre-oil window, with values of vitrinite reflectance (VR_o%) ranging between 0.41% and 0.55%, and the values of T_{max} between 409 °C and 443 °C. Optical microscopy with reflected white light and fluorescence blue light was used for identification of terrigenous macerals (vitrinite, liptinite as, resinite, cutinite, sporinite, and inertinite) associated with marine liptinite macerals (telalginite and lamalginite) showing yellow and bright–yellow epifluorescence.

Keywords: organic matter; macerals; kerogen; Upper Badenian; thermal maturity source rocks; Southern Carpathians; Romania

check for updates

Citation: Ghiran, M.D.; Popa, M.E.; Mariş, I.; Predeanu, G.; Gheorghe, Ş.; Bălănescu, N.M. Thermal Maturity and Kerogen Type of Badenian Dispersed Organic Matter from the Getic Depression, Romania. *Minerals* **2023**, *13*, 202. https://doi.org/10.3390/min13020202

Academic Editor: Thomas Gentzis

Received: 31 December 2022
Revised: 26 January 2023
Accepted: 27 January 2023
Published: 30 January 2023

1. Introduction

The Getic Depression occurs in the foreland of the Southern Carpathians, an important geological unit of Romania with numerous oil fields between the Danube and Dâmboviţa Valley. A limited number of studies on the use of organic petrology for the thermal maturity evaluation of the Getic Depression was published. This work addresses the maturity of Badenian source rocks of the Getic Depression (central-southern part) following the previous research of the immature Oligocene source rocks of Getic Depression (central-western part) done by [1]. The current research continues and completes previous geological assessments dealing with the basin with new organic petrology data.

In the area of the Getic Depression investigated by the authors, the generation and expulsion of hydrocarbons took place in two separate areas: a central-southern area and an eastern area [2–9]. In the central - southern area, where the maximal depths were reached, the oil generation occurred from Eocene and Lower Oligocene (Rupelian) formations during the late Oligocene (Chattian) in pelitic rocks, while the oil expulsion began in the early Burdigalian. In the eastern area, where the Oligocene formations occur at shallower depths, the generation and expulsion began in the early Miocene from Burdigalian formations and continues today [4,6,7,10].

For several decades the distribution and type of petroleum prospects based on the evaluation of petroleum source rocks, hydrocarbon generation potential estimation and oil & gas fields identification were undertaken [2–20].

The ways of evaluating the characters of the source rocks are well established worldwide, such as:

1. assessment of the level of thermal maturity and the amount of organic matter and type of kerogen [21–31].
2. microscopic identification of hydrocarbons source rocks, using thermal alteration index and vitrinite reflectance [21,25,27–30,32–37].

The colors differences of organic matter induced by thermal changes can be observed in transmitted and fluorescent light, aiding the identification of the phytoclast alteration rank on a 1 to 5 scale of the thermal alteration index (TAI, [21,37]).

The thermal alteration provides the organic matter color changing [21,37]. Total organic matter (TOC) content commonly assesses the amount of organic matter in a rock sample.

The maturation parameters such as temperature (T_{max}) and production index (PI), resulted from the Rock—Eval pyrolysis associated with vitrinite reflectance (VR_o%), allow to assess the stage of maturation [23,32,38–45].

The thermal maturity of organic matter increases with temperature, as it converts and further expels hydrocarbons during diagenesis, catagenesis, and metagenesis [21,32,37,46–57].

With the aim to express thermal maturity and determination of kerogen type from the perspective of organic petrology, the correlation between dispersed organic matter microscopy and geochemical analysis is detailed, combining geological and petrographical approaches with statistical approaches applied to Badenian source rocks of the Getic Depression. The vitrinite reflectance was measured and the types of macerals in reflected and fluorescent light were identified. Fluorescent properties of the liptinite macerals were proven to be an important distinguishing feature leading to the identification of the kerogen types and hydrocarbons generation potential of the selected samples.

Therefore, it is possible to outline the Getic Depression and to assess the organic facies in this area. The results obtained on the core samples from the Institute of Research and Technological Design I.C.P.T. Câmpina—OMV PETROM S.A. are going to be useful both nationally and internationally, due to the significance of the organic matter identified in the studied source rocks of Romania, in the frame of their wider stratigraphic, European context.

2. Geological Setting

The Getic Depression is developed as a narrow sedimentary basin, elongated from west to east, between the South Carpathians Orogen in the north and the Moesian Platform in the south, the Dâmbovița Valley in the east and the Danube River in the west (Figure 1), [58–60].

The tectonic evolution of the Getic Depression was marked by a northward continuous subduction movement of the Moesian Platform beneath the South Carpathians Orogen. Since the moment of its formation as a sedimentary basin during the Eocene, the Getic Depression recorded three significant orogenetic phases: the Saavic (at the end of Oligocene), Styrian (extension/transpression during the Palaeogene until the Lower Miocene) and Moldavian (deformations during the middle to late Miocene) [58–62].

Previous authors [63–72] detailed the strike-slip evolution of the basin during the Palaeogene to the early Miocene. These strike-slip deformations were mainly generated during the early Miocene, related to the movement and rotation of the Inner Carpathians over the Moesian Platform [62,66,71,72].

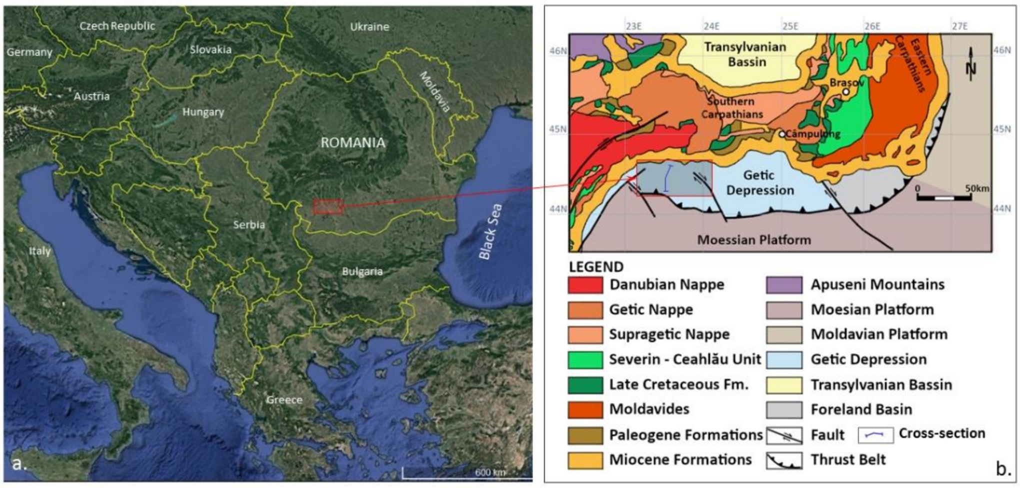

Figure 1. (**a**) Occurrence of the studied area (Google Earth source); (**b**) Simplified tectonic map of the Getic Depression, and of the South and East Carpathians, with the studied area marked as rectangular figure. Modified from [58,66,69].

The Getic Depression accumulated sediments which were transported southwards from the Carpathians chain, showing a fining upward general trend [58–60]. The almost entirely clastic succession was interrupted by evaporites (as local interlayers of anhydrite and salt in Aquitanian, Burdigalian and Badenian) during the early Burdigalian and the Badenian, while the mountain belt in the north was continuously uplifted during the geological evolution of the Getic Depression, beginning with the Eocene, and ending during the Pliocene (Romanian, Figures 2 and 3).

Since the Eocene, marine conditions occurred throughout the entire Getic Depression. The Eocene sediments lay unconformably and transgressively over the Cretaceous and Jurassic formations, including conglomerates, coarse and fine sandstones in the west and with interlayers of marls in the rest of the region (Figure 2, [59,60]).

During the Oligocene, the marine environment was anoxic, with deep sea episodes, the basin acquiring an asymmetrical and narrow shape, elongated along a west—east trend. A strong subsidence occurred in the central part of the basin, concurrently with a strong uplift of its northern margin, while the erosion process of the Mesozoic crystalline formations and of the Eocene deposits was activated. During the late Oligocene, the sea extended to the north, beyond the outcrops along the Getic Depression's margin [59,60].

The Miocene formations lay conformably over the Oligocene. During the Burdigalian, two distinct sedimentation cycles were recorded, the early Burdigalian and the late Burdigalian sequences as the sea covered most of the Getic Depression. The Lower Burdigalian sediments include marly sandstones, locally conglomeratic, with marls and shales rarely associated with thin anhydrite interlayers and a salt bearing sequence. The climate was arid and the accumulation of evaporites was possible. In the eastern part of the Getic Depression, the Lower Burdigalian occurs as local salt and anhydrites sequences. The Upper Burdigalian deposits occur transgressively overlaying older formations, starting with a sequence with coarse sandstone, conglomerate, and marl interlayers (100–1000 m), followed by a marly-sandstone sequences (400–600 m), and ending with sandstone (500–600 m). The Upper Burdigalian sequence was influenced by a marine phase, with a strong freshwater phase to its top. The water freshening was related to the water supply from the continent, inducing a brackish fauna [60]. In the eastern part of Getic Depression, the thickness of Upper Burdigalian is reduced due to the partial non-deposition of the lower sandy complex and to strong erosion [60].

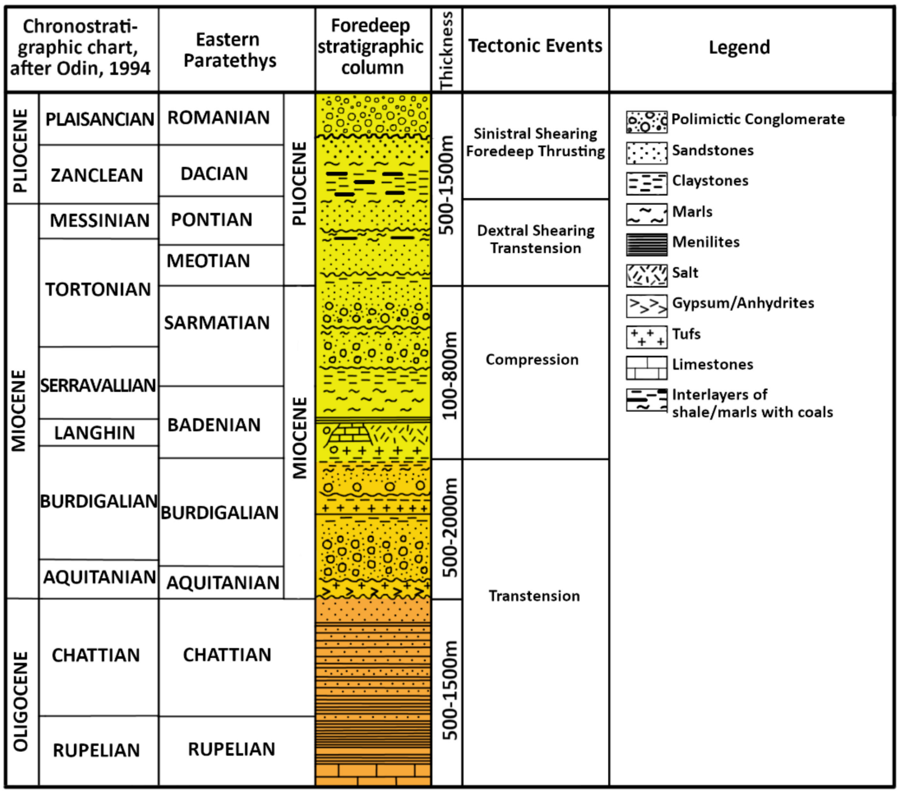

Figure 2. Stratigraphic log of the Getic Depression, Romania, simplified after [60].

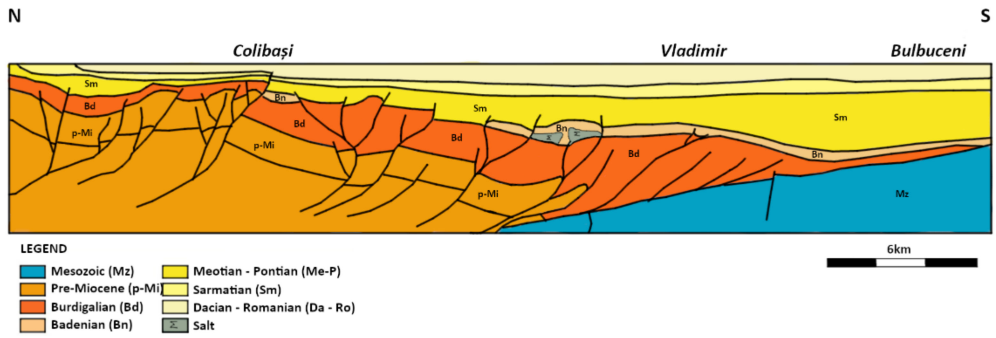

Figure 3. N–S Geological cross-section of the Getic Depression through Colibași–Vladimir–Bulbuceni structures. Modified from [61].

The Badenian sequence lays unconformably over the Burdigalian (Figures 2 and 3), with the same spreading area during the Sarmatian. The Badenian stratigraphy of the Getic Depression is marked by four horizons corresponding to a sedimentary transition from deep marine to epicontinental conditions:

1. the *Globigerina*-bearing tuffs and marls (Lower Badenian).
2. the salt breccia (Upper Badenian), with gypsum interlayers.
3. the radiolaria-bearing shales.
4. the *Spiratella*-bearing marls (ending the Badenian).

The depositional and geochemical evolution of the Getic Depression during the Badenian was not standard, with lots of geochemical changes, with sediment-starved, remanent basins controlled tectonically. The depositional shift was frequent, therefore in the sediment-starved basins fine sediments (as the shales with radiolarians) were deposited, although the depths were getting shallower continuously.

All these levels correspond to a deep marine—epicontinental environment [60], marked by the *Orbulina* (Lower Badenian) and *Valapertina* (including the assemblage with *Sphaeroid-*

ina bulloides, Upper Badenian) foraminiferal biozones. To these foraminiferal assemblages are added the nannoplanktonic assemblages with *Discoaster exilis* (Lower Badenian) and *Helicosphaera minuta* (Upper Badenian) and the palynological assemblages with *Nemathosphaeropsis* and *Svalbardella* (entire Badenian). The tuffs and marls with *Globigerina* were locally identified in wells, although their thickness varies strongly due to non-deposition or erosion.

The salt breccia crossed by wells occurs in structurally lower areas (Vladimir and Grădiște), and these horizons yields locally gypsum interlayers. The thickest Badenian deposits occur in the southern and western parts of the Getic Depression, while they disappear eastwards over large areas. The transition from marine to brackish environments occurred during the Sarmatian.

The tectonic movements of the Moldavian (Attic) paroxysmal phase generated the southward thrust of the Getic Depression over the Moesian Platform. These movements occurred during the whole Sarmatian with structural uplifts, especially in the western part of the Getic Depression.

The western part recorded continuous downward movements, generating thick sequences of Sarmatian and Badenian deposits, while in the eastern part, due to the uplift movements, these deposits are missing on large areas.

The Sarmatian deposits include sandstones, sand, and grayish marl layers, variable in thickness. The Maeotian deposits are predominantly pelitic, with marls, thin sands, and sandstones, influenced by proximal shelf conditions with brackish, mesohaline, dynamic waters. The Pontian deposits conformably overlay the Maeotian sequences, with marls and sandy marls, while the Pontian-Dacian-Romanian sequences include sandstones and marls, with coal seams [60] (Figures 2 and 3).

3. Materials and Methods

The samples were selected from borehole cores having their repository with the Institute of Research and Technological Design I.C.P.T. Câmpina—OMV PETROM S.A. A total of 33 Badenian core samples from 21 wells belonging to 14 structures were studied for the hydrocarbon's generation potential and for their organic geochemical and petrographical features (Table 1). Organic-rich, black shales and marls samples occurred on the following structures: Socu, Totea, Hurezani, Vladimir, Piscu Stejarului, Bibești, Bibești-Bulbuceni, Bulbuceni, Logrești, Drăganu, Grădiște, Colibași, Rădinești and Budieni (Figure 4).

A series of wells yield single core samples from Upper Badenian sequences (A-1 Grădiște, A-1 Drăganu, A-1 Budieni, A-1 Colibași, and A-1 Rădinești). They were relevant for the Upper Badenian from depths between 2200–2900 m. The Upper Badenian is thin, therefore, supplementary samples could not be probed.

Samples preparation was performed in accordance with SR ISO 5069-2: 1994 [73].

The microscopic studies on dispersed organic matter were performed on polished blocks to identify petrographic composition, and vitrinite reflectance. For preparation of pellets for the microscopical study, samples with various lithologies, from clays with poorly consolidated siltstone, claystone to marly siltstone were embedded in epoxy resin and polished with different grain sizes of carborundum paper and alumina according to ISO 7404-2: 2009 [74]. The vitrinite reflectance analysis was performed in accordance with ASTM D7708-11: 2014 [75] methodologies. The highest number of vitrinite reflectance measured points was 30. The standard deviation is between 0.03 and 0.08.

The pellets were analyzed using an Olympus BX50 optical microscope, equipped with a 50× oil immersion objective and a Tidas photometer MSP 200 Vers. 3.47. Ro, calibrated against the Sapphire reflectance standard (0.594% Ro) for vitrinite reflectance measurements. For the Rock-Eval analysis (conducted on duplicate samples), about 70 mg of each selected core sample was crushed, sieved, and weighed into a steel crucible [76]. A Rock-Eval 6 equipment was used to investigate the type of kerogen, thermal maturity, source rock potential, and generated hydrocarbons. The guidelines provided by [25–27,41] were followed in interpreting the results.

Table 1. Geochemical results of Rock-Eval analysis and vitrinite reflectance of Badenian Source Rock from Central-Southern part of the Getic Depression. Abbreviations and Acronyms: VRo%—measured vitrinite reflectance; TOC—total organic carbon of the rock sample, automatically calculated and recorded in weight ratio (wt.%); S_1—amount of free hydrocarbons from the rock samples (mg HC/g rock); S_2—remaining hydrocarbons generation potential of the source rock (mg HC/g rock); S_3—oxygen compounds, amount of CO_2 from organic source (mg CO_2/g rock); Tmax-temperature of maximum hydrocarbon generation from a rock sample during pyrolysis analysis (°C); HI—Hydrogen Index (HI = S_2/TOC)—the amount of hydrogen relative to the amount of organic carbon present in a sample (mg HC/g TOC); OI—Oxygen Index (OI = S_3/TOC)-the amount of oxygen relative to the amount of organic carbon present in a sample (mg CO_2/g TOC); PI—Production Index = $S_1/S_1 + S_2$; S_2/S_3 ratio-oil or gas generation potential. Petrographyc composition: H—huminite; V—vitrinite; L—liptinite; S—sporinite; C—cutinite; R—resinite; Lag—lamalginite; Tag—telalginite; Ts—Tasmanites; Pr—other Prasinophyceae; Ls—Leiosphaeridia; Ld—liptodetrinite; I—inertinite; F—fusinite; In—inertodetrinite; Py—pyrite; Sd—siderite; B—bioclasts.

No.	Well	Depth, m	TOC wt.%	S_1, mg HC/g rock	S_2, mg HC/g rock	S_3, mg CO_2/g rock	T_{max}, °C	HI, mg HC/g TOC	OI, mg CO_2/g TOC	PI (S_1/(S_1+S_2)	S_2/S_3	VRo, %	Standard Dev.	Petrographic Composition	Kerogen Type	Generation Potential
1	A-1 Grădiște	2200–2300	1.82	0.23	3.74	1.25	409	206	69	0.06	3.00	0.47	0.05	V, Lag, Tag, R, In, Py, Sd, B	III	gas
2	A-1 Drăganu		0.41	0.01	0.13	0.74	430	32	180	0.07	0.18	0.45	0.04	V, I, Sd, B	IV	poor
3	A-1 Colibași	2600–2700	0.07	0.01	0.01	0.93	433	14	211	0.05	0.01	0.49	0.03	V, Tag (Pr), Py	IV	poor
4	A-1 Rădinești	2700–2800	1.35	0.14	2.01	0.73	419	150	55	0.07	2.75	0.41	0.07	V, C, S, Tag (Pr, Ls), Py	III	gas
5	A-1 Budieni	2800–2900	0.59	0.07	0.6	0.26	423	102	44	0.11	2.31	0.42	0.05	V, Lag, Tag (Pr, Ls), I, Py	III	gas
6	A-1 Hurezani	3000–3100	0.89	0.06	1.05	0.45	434	118	51	0.05	2.33	0.42	0.05	V, C, R, S, Tag (Ts, Pr), F, Py, Sd	III	gas
7	B-1 Hurezani	3100–3200	0.99	0.03	1.02	0.87	430	103	88	0.03	1.17	0.46	0.03	V, S, C, Tag (Ts, Ls, Pr), Ld, I, Py, Sd	III	gas
8	B-1 Socu		0.68	0.02	0.66	0.64	430	97	94	0.03	1.03	0.44	0.03	V, Lag, Tag (Ts, Pr), R, S, Py, Sd	III	gas
9	A-2 Hurezani		1.20	0.06	1.61	0.52	433	134	43	0.04	3.10	0.48	0.04	V, Ld, Py, Sd	III	gas
10	A-1 Totea		0.81	0.04	1.23	0.75	433	152	92	0.03	1.64	0.52	0.03	V, S, Tag (Pr, Ls, Ts), I, Py	III	gas
11	C-1 Socu		0.54	0.02	0.55	0.81	435	103	150	0.03	0.68	0.49	0.04	H/V, Tag (Ts, Pr, Ls), R, S, Py	IV	poor
12	D-1 Socu		0.5	0.03	1.25	0.96	433	272	195	0.03	1.30	0.47	0.04	V, Tag (Ts, Ls, Pr), R, I, Sd, B	III	gas
13	D-2 Socu		0.39	0.01	0.4	1.06	435	103	278	0.02	0.38	0.46	0.04	V, Tag (Ts, Ls, Pr), S, I, Py	IV	poor

Table 1. *Cont.*

No.	Well	Depth, m	TOC wt.%	S_1, mg HC/g rock	S_2, mg HC/g rock	S_3, mg CO_2/g rock	T_{max}, °C	HI, mg HC/g TOC	OI, mg CO_2/g TOC	PI (S_1/(S_1+S_2))	S_2/S_3	VRo, %	Standard Dev.	Petrographic Composition	Kerogen Type	Generation Potential
14	A-2 Colibași	3200–3300	0.48	0.02	0.24	1.08	429	50	255	0.08	0.22	0.52	0.04	V, Tag (Ls, Pr), Ld, S, Py	IV	poor
15	C-2 Socu		1.04	0.07	1.15	0.83	434	111	80	0.05	1.39	0.44	0.06	V, S, Tag (Ts, Pr), Py, Sd	III	gas
16	A-1 Vladimir		1.08	0.05	1.09	0.93	432	101	86	0.04	1.17	0.48	0.03	V, Tag (Pr, Ls), S, R, Py	III	gas
17	A-1 Socu		0.55	0.03	0.43	0.55	437	78	100	0.07	0.78	0.54	0.04	H/V, Tag (Ts, Pr, Ls), S, R, Ld, I, Py, Sd, B	IV	poor
18	D-3 Socu		0.52	0.02	0.8	0.87	435	154	168	0.02	0.34	0.52	0.05	V, Tag (Ts, Ls, Pr), R, I, Py	IV	poor
19	A-3 Colibași	3400–3500	0.31	0.03	0.2	0.32	435	65	103	0.13	0.63	0.52	0.04	V, Tag (Ls, Pr), Sd, B	IV	poor
20	B-1 Totea		1.43	0.07	2.07	1.07	433	145	75	0.03	1.93	0.48	0.04	V, Tag (Ts), Py	III	gas
21	A-1 Logrești	3500–3600	0.49	0.02	0.4	0.96	430	82	196	0.05	0.42	0.46	0.04	V, Lag, Tag (Pr), S, Py, Sd	IV	poor
22	A-1 Piscu Stejarului	3600–3700	0.61	0.03	0.54	1.04	437	88	171	0.05	0.52	0.52	0.05	V, Tag (Ts, Pr), Lag, R, F, Py, Sd	IV	poor
23	A-2 Piscu Stejarului	3800–3900	0.83	0.12	1.41	0.95	442	177	115	0.08	1.48	0.55	0.04	V, Tag (Ts, Pr), Lag, Lp, S, R, I, Py, Sd	III	gas
24	A-1 Bibești	3900–4000	0.51	0.05	0.46	0.21	440	90	41	0.1	2.19	0.44	0.04	V, Tag(Ts, Ls, Pr), L(S, R), I, Py, Sd	III	gas
25	A-1 Bulbuceni		0.43	0.04	0.28	0.27	437	65	63	0.13	1.04	0.5	0.04	V, Lag, L(S), Tag (Pr, Ts, Ls), Py, Sd	III	gas
26	A-1 Bib-Bulbuceni	4000–4100	0.51	0.05	0.35	0.26	440	69	51	0.13	1.35	0.48	0.03	V, Tag (Ls), L(S), Py	III	gas
27	A-2 Bib-Bulbuceni		0.59	0.06	0.52	0.21	443	88	36	0.01	2.48	0.48	0.04	V, Tag (Ls, Pr, Ts), Lp, S, R, I, Py	III	gas
28	A-3 Bib-Bulbuceni		0.47	0.04	0.35	0.19	441	74	40	0.01	1.84	0.49	0.04	V, Tag (Ls, Ts), Lp, L(S, R), I, Py	III	gas
29	A-2 Bibești		1.04	0.11	2.13	0.41	436	205	39	0.05	5.19	0.45	0.03	V, Tag (Ts, Pr, Ls), R, S, Py	III/II	gas and oil

Table 1. *Cont.*

No.	Well	Depth, m	TOC wt.%	S_1, mg HC/g rock	S_2, mg HC/g rock	S_3, mg CO_2/g rock	T_{max}, °C	HI, mg HC/g TOC	OI, mg CO_2/g TOC	PI (S_1/(S_1+S_2))	S_2/S_3	VRo, %	Standard Dev.	Petrographic Composition	Kerogen Type	Generation Potential
30	A-3 Bibești	4100–4200	0.62	0.06	0.56	0.2	443	90	32	0.1	2.80	0.48	0.06	V, Tag (Ts), Lag, Lp, R, S, I, Py, Sd	III	gas
31	B-1 Bulbuceni		1.01	0.22	1.86	0.45	442	184	45	0.11	4.13	0.44	0.06	V, Tag (Ts, Ls), Lag, Lp, L(S, C), Py, B	III	gas
32	B-2 Bulbuceni	4300–4400	0.57	0.04	0.51	0.24	439	89	42	0.07	2.13	0.5	0.08	V, Tag (Pr), Lag, Ld, I, Py, Sd	III	gas
33	C-1 Bulbuceni		0.55	0.08	0.93	0.28	440	169	51	0.08	3.32	0.51	0.05	V, Tag (Ts), Ld, Py	III	gas

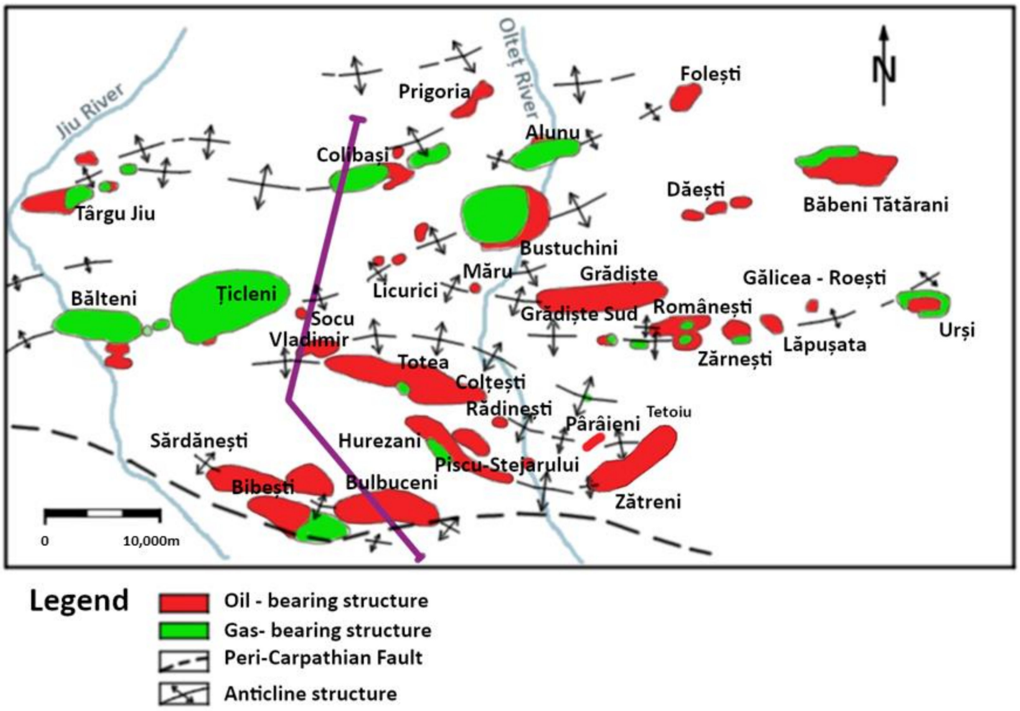

Figure 4. Map with Miocene oil and gas fields. Selected perimeter with structures and cross-section (Figure 3) of the center-southern part from the Getic Depression. (OMV PETROM S.A.-I.C.P.T. Câmpina).

The classifications developed by the International Committee for Coal and Organic Petrology for vitrinite [77], liptinite [78]), huminite [79]) and inertinite [80] were used.

4. Results and Discussions

4.1. Petrology of the Dispersed Organic Matter

The vitrinite reflectance measurements and Rock-Eval results are given in Table 1.

In the Upper Badenian samples, macerals such as vitrinite, liptinite (sporinite, resinite, cutinite), and inertinite are integrated with marine liptinite macerals (acritarchs) such as: telalginite, lamalginite and liptodetrinite. Qualitative petrographic composition was carried out, and it is presented as macerals and minerals in Table 1. Vitrinite is frequent in all samples, and it is associated with a variety of liptinite macerals (Figures 5–7). Cutinite is accompanied by sporinite, which is yellow in fluorescent light (A-1 Socu, A-3 Colibași, A-1, B-1 Hurezani, B-1 Bulbuceni, B-2, 3 Bibești) (Figure 7). Resinite occurs mostly as globular bodies, golden-yellow to brownish—yellow in epifluorescence (D-1 Socu, A-1, 2, 3 Bibești). Inertinite is rare and was identified in the following wells: A-1 Budieni, A-1 Hurezani—fusinite; B-2 Bulbuceni—funginite.

Alginite as telalginite is related to algae such as *Tasmanites*, *Leiosphaeridia* and other Prasinophyceae, and it was identified using optical microscopy following the ICCP classifications [78], [81–83]. Alginite shows a variable fluorescence emission intensity ranging from green-yellow to bright yellow (A-1 Socu, B-1 Socu, C-2 Socu, A-1, 2 Piscu Stejarului, A-1 Totea, B-1 Totea, A-1 Bulbuceni, B-2 Bibești—Bulbuceni, A-1 Rădinești, A-1 Budieni) (Figure 5).

Alginite as lamalginite was identified only in A-2 Piscu Stejarului, C-2 Socu, A-1 Logrești, A-1 Grădiște, and A-1 Budieni wells, A-1 Bulbuceni, A-3 Bibești and B-1 and B -2 Bulbuceni with irregular shapes, with a lack of internal structure and having a lower fluorescence intensity than the telalginite.

Spores were identified in most of wells, accompanied by resinite and cutinite: Socu, Totea, Hurezani, Vladimir, Piscul Stejarului, Bibești, Bibești-Bulbuceni, Bulbuceni, Logrești, and Rădinești (Figures 6–8), with TAI between 1^+ and 3^-.

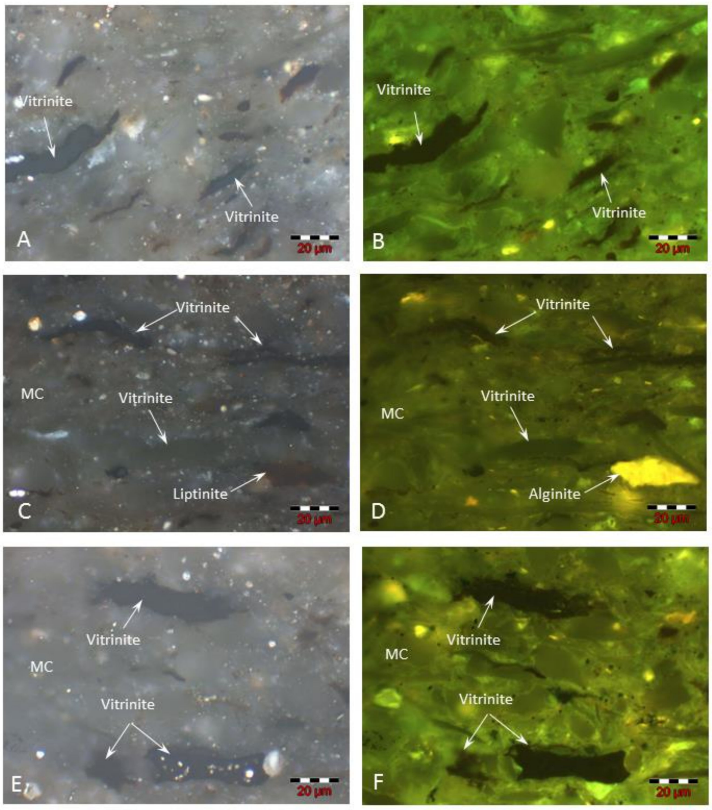

Figure 5. Photomicrographs of C-1 Socu Upper Badenian source rocks of the Getic Depression showing vitrinite associated with mixed, continental, and marine origins liptinite in a mineral groundmass with pyrite. Reflected light (RL: figures **A**,**C**,**E**) and fluorescence (FL: figures **B**,**D**,**F**), oil immersion, 500×. Py: pyrite, MC: mineral carbonate.

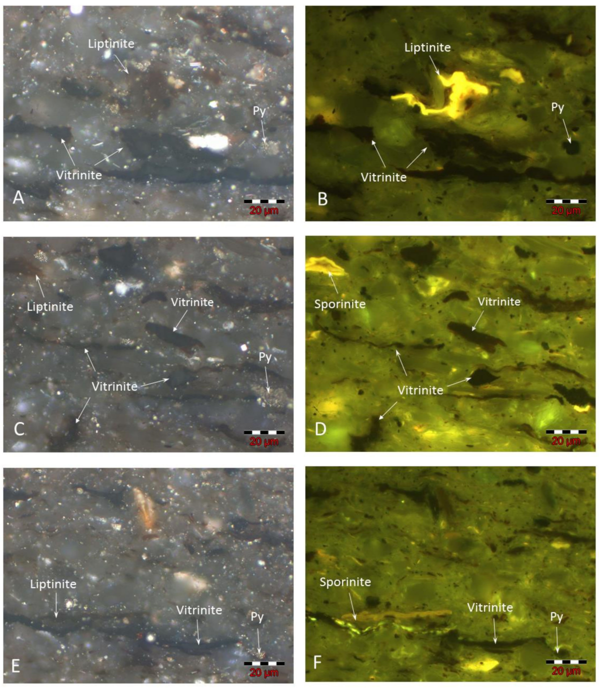

Figure 6. Photomicrographs of C-2 Socu Upper Badenian source rocks of the Getic Depression showing continental liptinite origin in a mineral carbonate groundmass with pyrite. Reflected light (RL: figures **A**,**C**,**E**) and fluorescent light (FL: figures **B**,**D**,**F**), oil immersion, 500×.

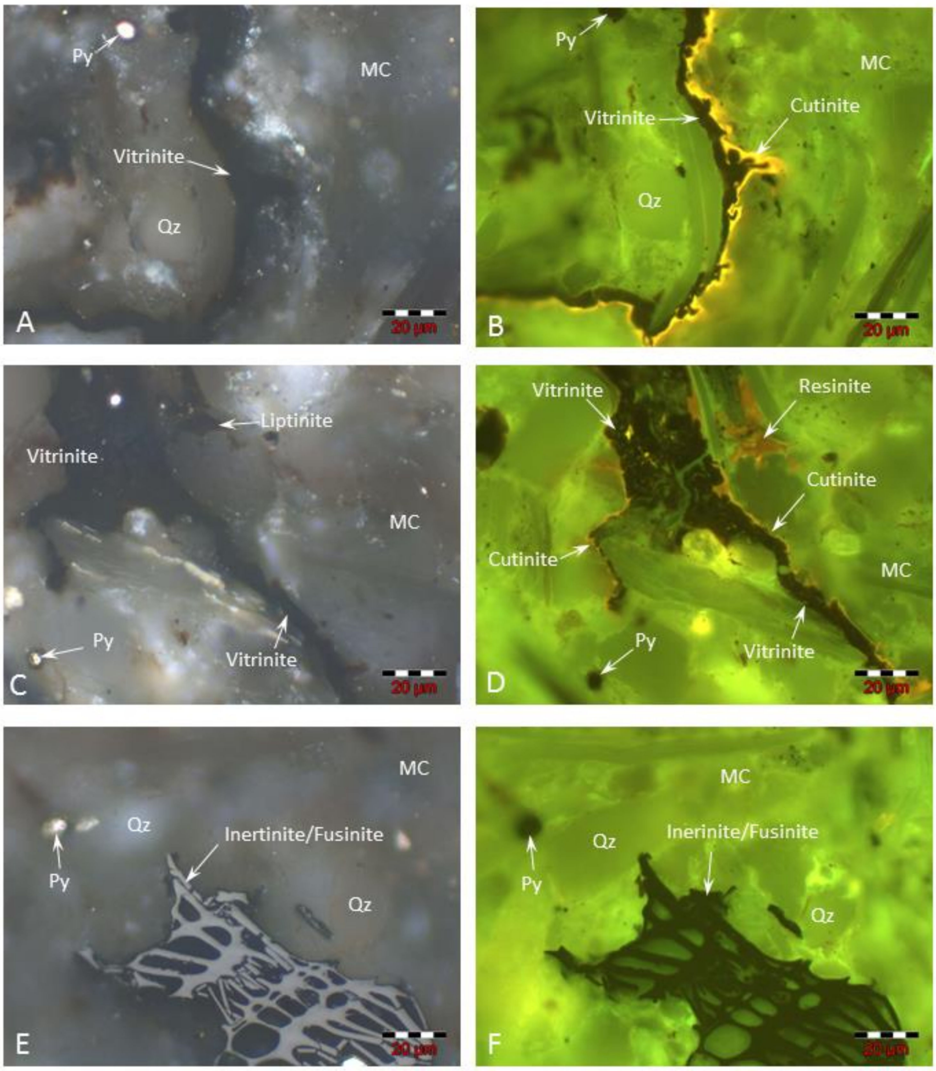

Figure 7. Photomicrographs of A-1 Hurezani Upper Badenian source rocks of the Getic Depression showing the continental origins of macerals in a mineral carbonate (MC) groundmass with quartz (Qz), and pyrite (Py). Reflected light (RL: figures **A**,**C**,**E**) and fluorescent light (FL: figures **B**,**D**,**F**), oil immersion, 500×.

Liptodetrinite with irregular shape shows increased fluorescence intensity in B-1 Bulbuceni, B-1 Hurezani, A-1, 3 Bibești, B-2, 3 Bibești and A-1 Rădinești samples. Although pyrite occurrence alone is not enough for demonstrating the anoxic conditions, it is an useful marker to assess depositional conditions. Thus, pyrite occurs generally as framboidal and dispersed, associated with iron carbonates (siderite) in Vladimir-Totea, Rădinești, Bibești, Bulbuceni showing anoxic conditions, and in Colibași, Socu, Logrești, Piscu Stejarului, Drăganu, structures showing oxic conditions (Figure 5C, Figure 6A,E and Figure 8E,F).

Bioclasts occur in Upper Badenian samples (A-1 Socu, D-1 Socu, A-1 Piscu Stejarului, A-3 Colibași, B-1 Bulbuceni, A-1 Drăganu, A-1 Grădiște), but occasionally, bioclasts show the frequent pyrite inclusions (A-1 Vladimir).

The random vitrinite reflectance (VR_o%) ranges between 0.41% and 0.55%, with T_{max} values between 409 °C and 443 °C (Figures 9 and 10), both parameters suggesting that the organic matter maturity varies from thermal immaturity to very early oil maturity.

The values of measured vitrinite reflectance (VR_o%), thermal alteration index (TAI) and T_{max} show that 23 analyzed rock samples are immature, and the other 10 samples occur in the early maturity part of the oil window (Figures 9 and 10).

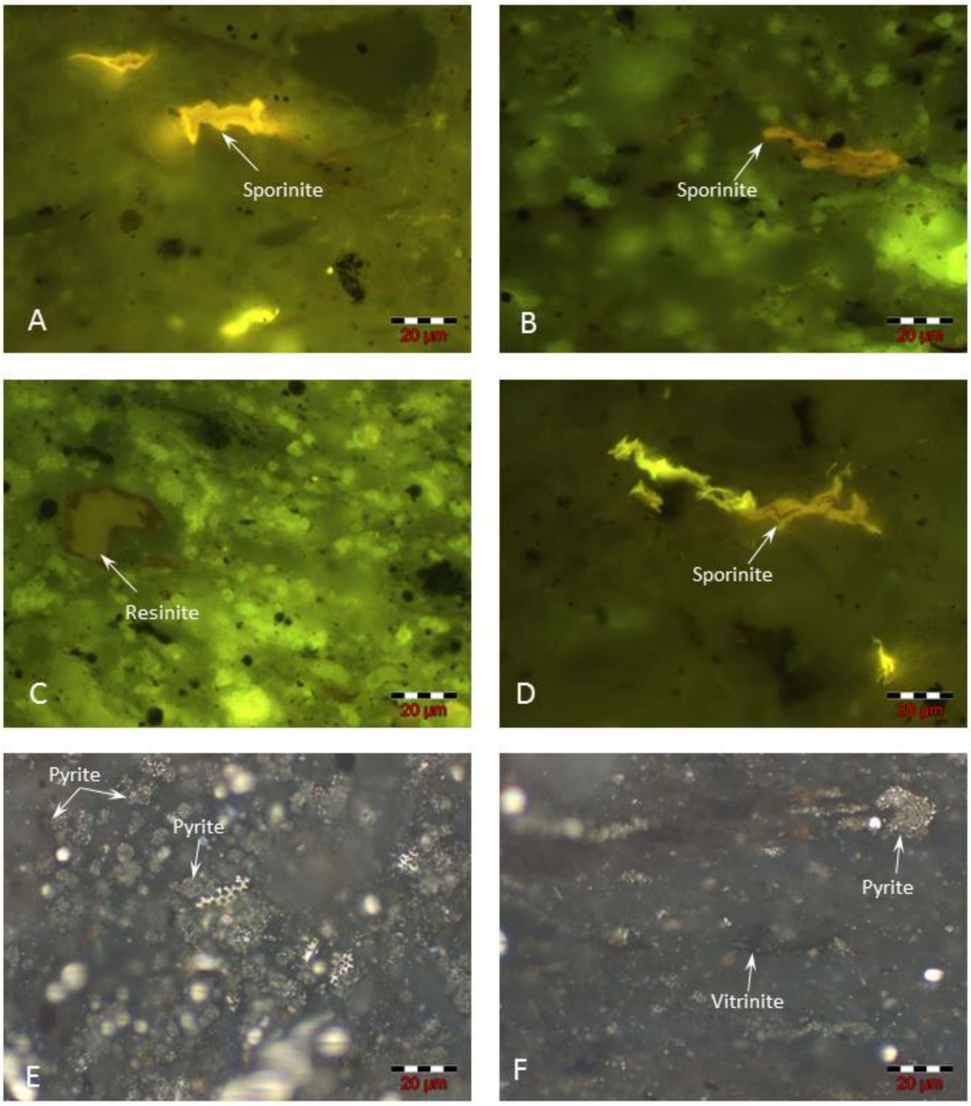

Figure 8. Photomicrographs of phytoclasts, altered spores (A-1, 2, 3 Bibești, A-1, 2, 3 Bibești—Bulbuceni, B-1 Bulbuceni) and pyrite nests (A-1 Vladimir, A-1,2 Totea, B-1 Totea and A-1 Rădinești), FL (**A**–**D**) and RL, (**E**,**F**), oil immersion, 500×, scale bar: 20 µm.

The Badenian samples show values of T_{max} and VR_o (%) (Table 1 and Figure 9) that help to group them as following:

a. T_{max} < 435 °C, VR_o < 0.50%, indicating immaturity (B-1, C-2, D-1 Socu, B-1 Totea, A-1, 2, B-1 Hurezani; A-1 Vladimir, A-1 Logrești, A-1 Drăganu, A-1 Grădiște, A-1 Colibași, A-1 Rădinești and A-1 Budieni).

b. $T_{max} \geq 435$ °C, VR_o% < 0.50%, indicating vitrinite values lower than expected (C-1 Socu, D-2 Socu, A-1, 2, 3 Bibești, B-1, 2, 3 Bibești—Bulbuceni and B-1 Bulbuceni).

c. $T_{max} \geq 435$ °C, $VR_o\% \geq$ 0,50%, indicating thermal maturity, in the very early part of the oil generation zone (A-1, D-3 Socu, A-1, 2 Piscu Stejarului, A-1, B-2, C-1 Bulbuceni and A-3 Colibași).

d. T_{max} < 435 °C, VR_o% > 0.50%, indicating T_{max} values lower than expected (A-1 Totea and A-2 Colibași).

The T_{max} parameter is influenced not only by the shape of S_2, but also by the type and quantity of organic matter, the lithological matrix, the lithology of the rock and by other factors [36,52,81]. The diagram of VR_o (%) vs. T_{max} (°C) (Figure 9), shows that the T_{max} values are very low, especially in samples from A-1 Grădiște, A-1 Budieni and A-1 Rădinești wells. The extent of T_{max} reduction tends to be higher in the early stage of hydrocarbon generation window (435 °C–440 °C) [84,85].

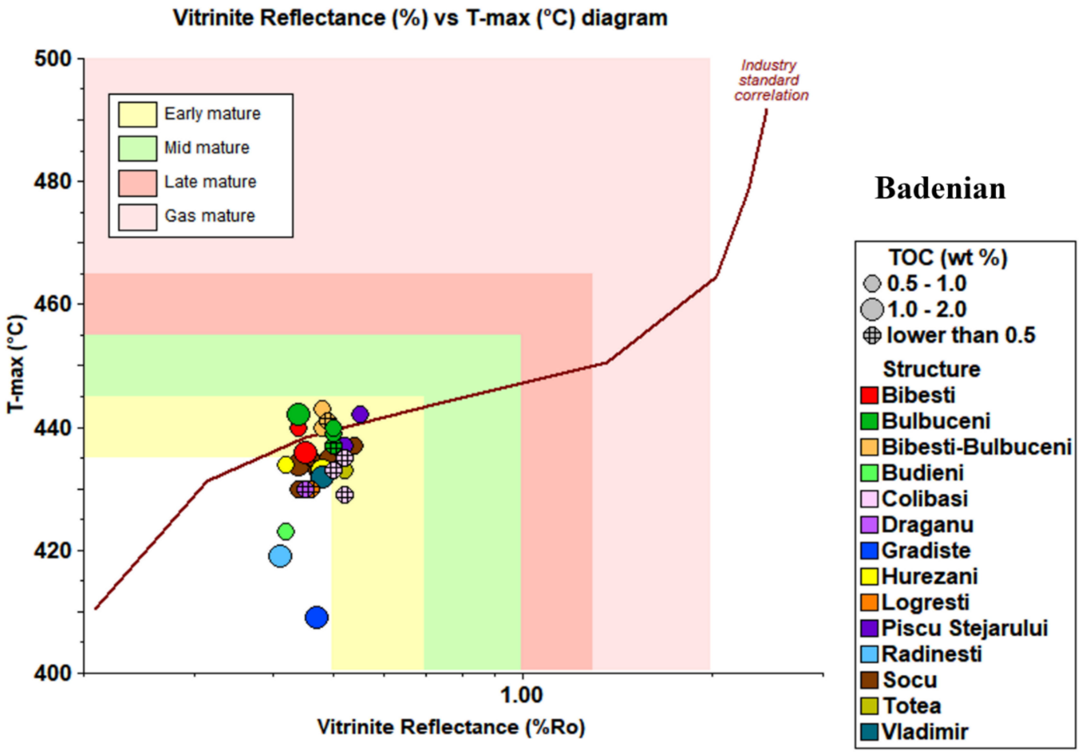

Figure 9. Vitrinite reflectance VR_o (%) vs. T_{max} (°C), showing the thermal maturity of the Upper Badenian source rocks from the central-southern part of the Getic Depression.

The low VR_o% values (Figure 10) first suggested vitrinite suppression. This process is linked to impregnation of vitrinite with hydrocarbons generated during kerogen maturation (not this case, as the thermal maturity is low), increased hydrogen content of vitrinite either as a result of a Hydrogen-rich matrix (lamalginite, bituminite) or of hydrogen-rich plant precursors. Both processes would result in high HI values (>400 mg HC/g TOC), and again, this is not the case in our dataset. Moreover, vitrinite reflectance variation may be linked to chemical differences in organic matter, possibly induced by diagenesis through syn- or post depositional degradation, occurring in sediments with clay minerals as catalysts. Differences in vitrinite reflectance are related to time-temperature history. The selected samples, deeper than 3500 m, from Bibești, Bibești-Bulbuceni, Bulbuceni, Piscu-Stejarului structures, have the most pronounced decrease of VR_o (%) and the highest values of the T_{max} (°C). As there is not enough evidence to argue the suppression of VR_o (%), the measured vitrinite reflectance values can be explained by retardation, as a possible mechanism for this group of samples, in the lack of overpressured sections and additional data required for such an interpretation.

The samples from A-1 Drăganu, A-1 Grădiște and A-1 Colibași wells show a normal variation of VR_o vs. depth. The possible retardation process in the Getic Depression was influenced by tectonic factors (extensions and transpressions) mentioned in Section 2.

T_{max} values are correlated with depth (Figure 11), although a group of samples have a slightly upward deviation from the theoretical variation, as the structures Socu, Colibași, Hurezani, Totea, and Vladimir have suffered uplift movements.

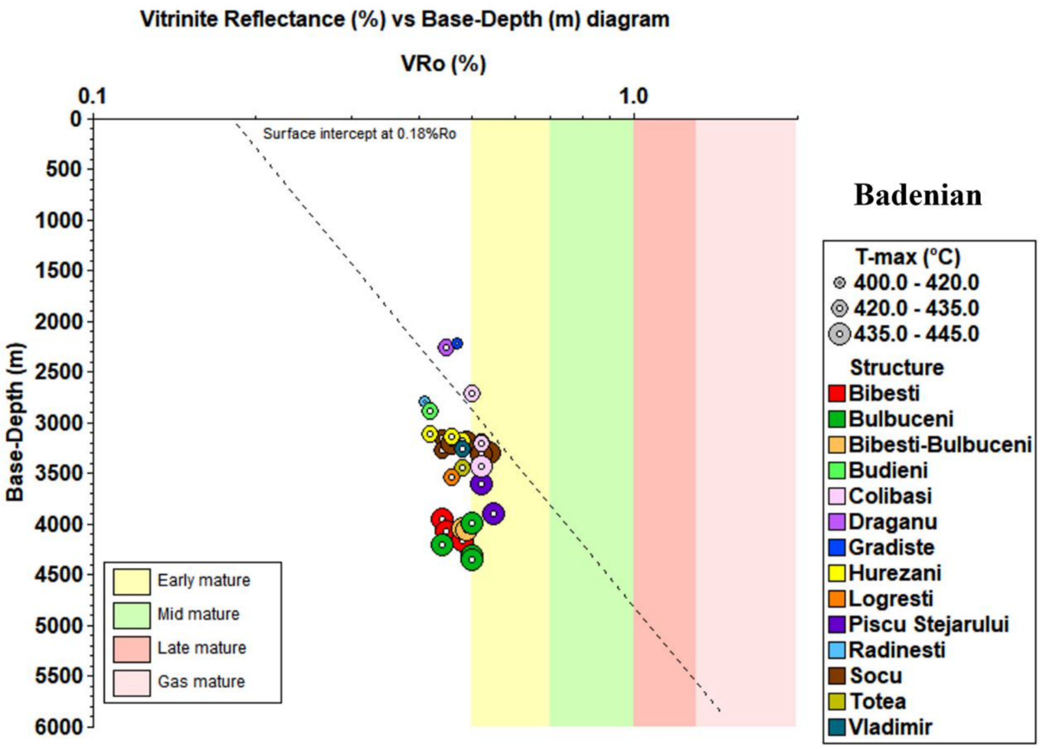

Figure 10. Vitrinite reflectance VR_o (%) vs. depth (m), showing the thermal maturity of the Upper Badenian source rocks from the central-southern part of the Getic Depression.

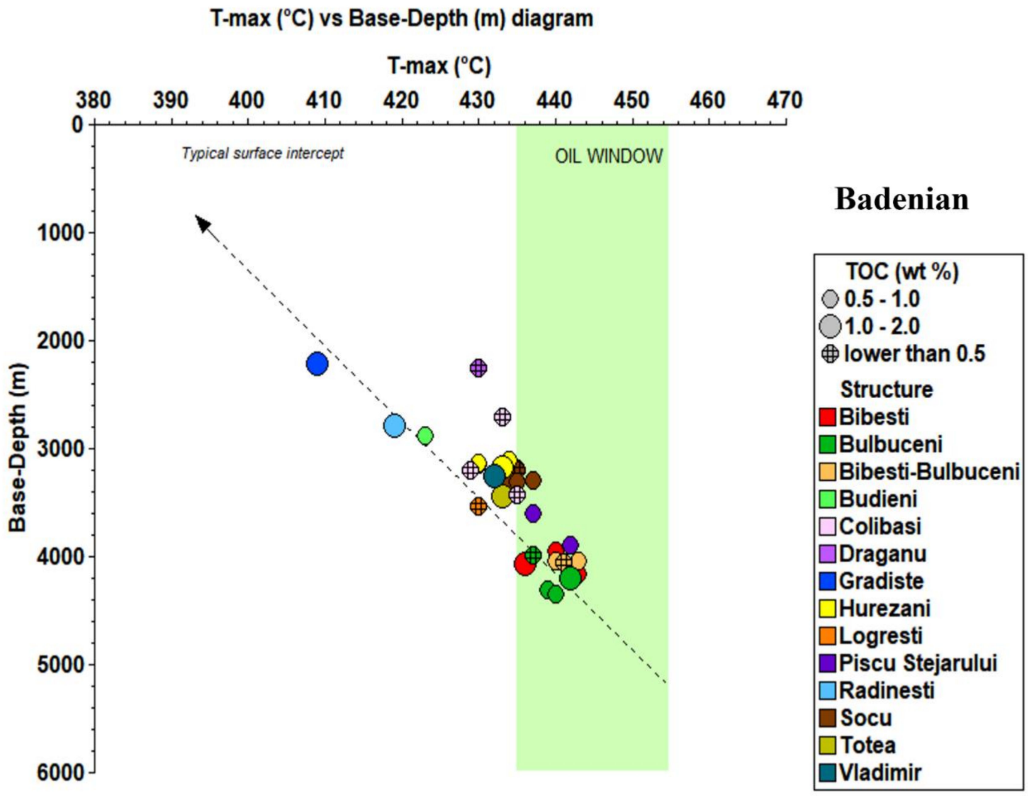

Figure 11. T_{max} (°C) vs. depth (m) diagram, showing the thermal maturity of the Upper Badenian source rocks from the central-southern part of the Getic Depression.

4.2. Geochemical Assessment

Depending on their TOC values and on their petroleum generation potential, the analyzed rock samples are split in three main groups (Figure 12, Table 1):

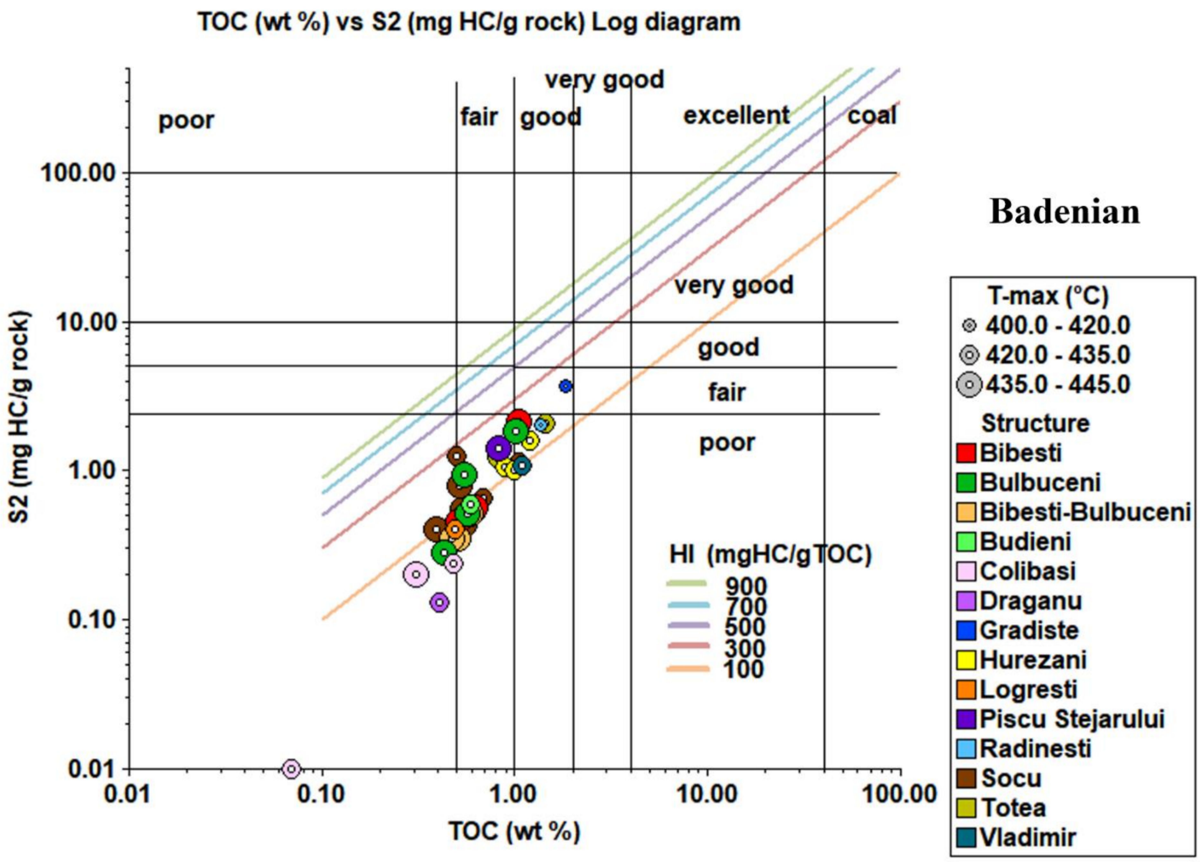

Figure 12. Hydrocarbon generation potential of Upper Badenian samples of the Getic Depression evaluated from TOC (wt.%) and S_2 (mg HC/g rock) parameters.

a. poor generation potential group, with TOC values between 0.07 wt.%. and 0.49 wt.% in D-2 Socu, B-3 Bibești—Bulbuceni, A-1 Bulbuceni, A-1 Logrești, A-1 Drăganu, and A-1, 2 and 3 Colibași wells.

b. fair generation potential group, with TOC values between 0.5 wt.% and 0.99 wt.% in A-1, B-1, C-1, D-1, D-3 Socu, A-1 Totea, A-1, B-1 Hurezani, A-1, 2 Piscu Stejarului, A-1, 3 Bibești, B-1, 2 Bibești Bulbuceni, B-2, C-1 Bulbuceni and A-1 Budieni wells;

c. good generation potential group, with TOC values between 1.01 wt.% and 1.82 wt.% in C-2 Socu, B-1 Totea, A-2 Hurezani, A-1 Vladimir, A-2 Bibești, B-1 Bulbuceni, A-1 Grădiște and A-1 Rădinești wells.

Based on the S_2 parameter, with values lower than 2.5 mg HC/g rock, the hydrocarbons generation potential is poor for 32 samples (Figure 13). Only a single sample from A-1 Grădiște well has S_2 of 3.74 mg HC/g rock and a fair hydrocarbons generation potential.

The values of Hydrogen Index (HI) in Upper Badenian samples range between 14 and 272 mg HC/g TOC, indicating a potential source for gas generating, type III kerogen (Table 1). In three samples from A-2 Bibești, D-1 Socu and A-1 Grădiște, HI values higher than 200 mg HC/g TOC were recorded only as these samples contain increased alginite and resinite macerals, type III/II, with a predominance of type III, generating mixed gas and oil, but mainly gas (Table 1, Figure 13).

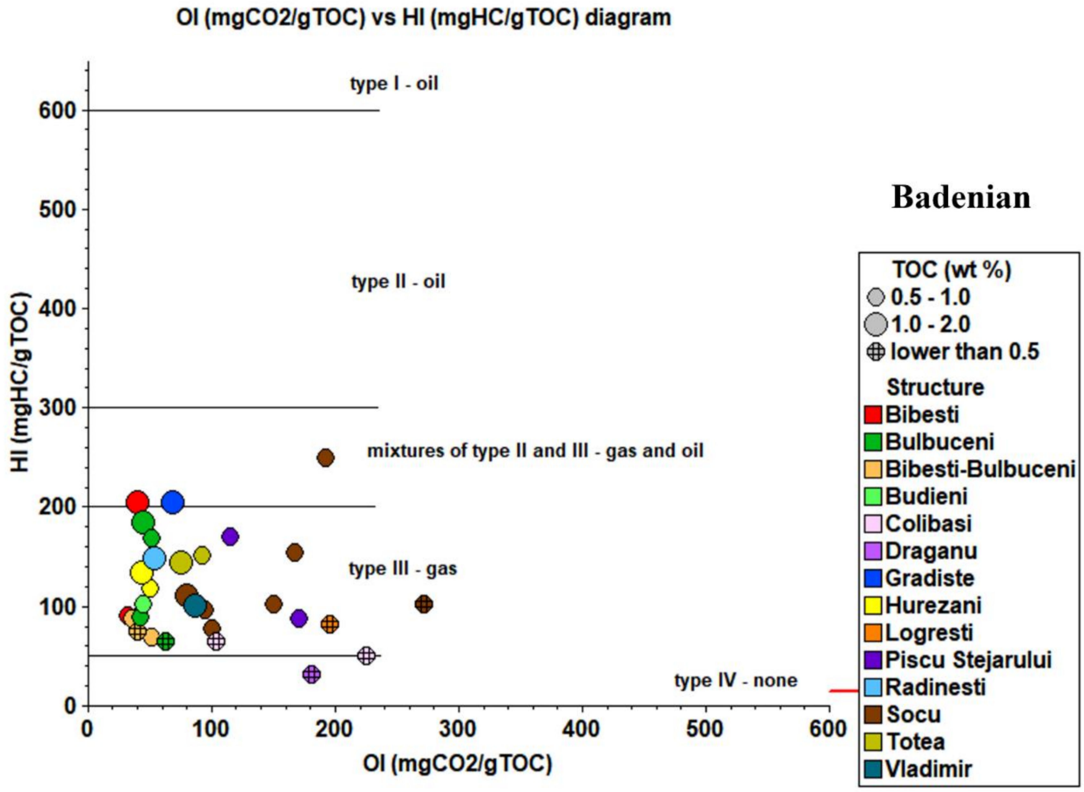

Figure 13. Oxygen Index (OI) (mg CO_2/g TOC) vs. Hydrogen Index (HI) (mg HC/g TOC), in a modified Pseudo Van Krevelen diagram, showing the kerogen types of Upper Badenian samples from the Getic Depression.

In C-1, D-1, 2, 3 Socu, A-1 Piscu Stejarului, A-1 Logrești, A-1 Drăganu and A-1, 2 Colibași wells, the Oxygen Index (OI) values range from 150 to 278 mg CO_2/g TOC. OI values higher than 150 mg CO_2/g TOC are related to TOC values lower than 0.5 wt.% due to mineral matrix effects or to mineral decomposition during the pyrolysis procedure and they are an indicator for the terrestrial organic matter occurrence or for immature organic matter from all sources [25]. The A-1, 2 Colibași and D-2 Socu samples have high values of OI because of their low values of S_1, S_2, TOC, the sample showing oxidizing effects. The values of S_2/S_3 ratio lower than 5 indicate the type III kerogen, suitable for gas and condensate, and only one sample has a S_2/S_3 ratio higher than 5 which indicates a type II kerogen, suitable for oil (A-2 Bibești).

Another important pyrolysis parameter is the Production Index (PI, Table 1), influenced by the conversion of kerogen into free hydrocarbons, and by the ratio of S_1 to the sum of S_1 + S_2, [30]. This ratio is significant when it reaches values between 0.05 and 0.5 (oil window). The Upper Badenian samples have an average PI of 0.08, with a maximal value of 0.13, the analyzed samples being in the immaturity area or in the early maturity area from the oil generation window (Table 1, Figure 14).

Studies of [29,30] indicated a correlation between the pyrolysis data and the hydrocarbon generation potential values. Some authors [27] showed that T_{max} values less than 435 °C, measured vitrinite reflectance (VR_o%) less than 0.5%, together with thermal alteration index (TAI) between 1–2^+ show immature stages of organic matter. From the analyzed rock samples, 23 samples are immature, and other 10 samples occur in the early maturity state of the oil window (Table 1). The modified Pseudo Van Krevelen diagram, (Figure 13) confirms that the analyzed rock samples present the Type III of kerogen, indicating a gas-generation potential.

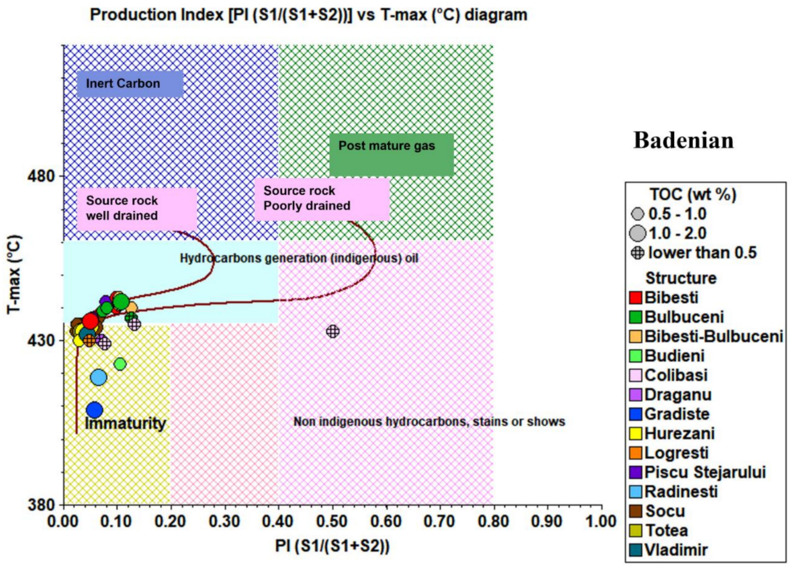

Figure 14. Production Index (PI) vs. T_{max} (°C) diagram, showing the hydrocarbon generation zone.

4.3. Statistical Analysis

For the identification of the potential correlation between the parameters, a preliminary statistical analysis of the datasets was performed (Table 2).

Table 2. Statistical parameters for all characters.

Statistical Parameter	TOC	S_1	S_2	S_3	T_{max}	HI	OI	PI	VR_o	S_2/S_3	Depth
Mean	0.723	0.058	0.925	0.645	434	113.939	101.181	0.080	0.478	1.673	3439.388
Standard Deviation	0.365	0.052	0.775	0.330	7.017	54.483	68.543	0.082	0.035	1.217	556.980
Minimum	0.070	0.010	0.010	0.190	409	14	32	0.020	0.410	0.010	2218
Maximum	1.820	0.230	3.740	1.250	443	272	278	0.500	0.550	5.190	4346.5
Confidence Level for mean (95.0%)	±0.129	±0.018	±0.275	±0.117	±2.488	±19.318	±24.304	±0.029	±0.012	±0.431	±197.496

The correlation coefficients (Table 3) indicate high correlation values between six parameters such as S_2 and TOC (0.918), S_1 and S_2 (0.820), T_{max} and Depth (0.807).

Table 3. The values of the correlation coefficients.

	TOC	S_1	S_2	S_3	T_{max}	HI	OI	PI	VR_o	S_2/S_3	Depth
TOC	1										
S_1	0.717	1									
S_2	0.918	0.820	1								
S_3	0.301	0.013	0.327	1							
T_{max}	−0.503	−0.285	−0.502	−0.513	1						
HI	0.554	0.581	0.760	0.206	−0.163	1					
OI	−0.430	−0.474	−0.335	0.690	−0.150	−0.182	1				
PI	−0.411	−0.065	−0.305	−0.134	0.091	−0.437	0.095	1			
VRo	−0.304	−0.257	−0.234	0.121	0.362	−0.102	0.244	0.076	1		
S_2/S_3	0.550	0.719	0.626	−0.435	0.045	0.566	−0.731	−0.150	−0.356	1	
Depth	−0.228	0.047	−0.205	−0.610	0.807	0.057	−0.418	−0.045	0.259	0.381	1

Background colors indicate the following variation ranges of correlation coefficients: orange: 0.6–0.7, light green: 0.7–0.8, green: 0.8–0.9, dark green: >0.9.

T_{max} and depth parameters dependency is described by a linear model (Figure 15) with a high adjusted R-squared value (0.651).

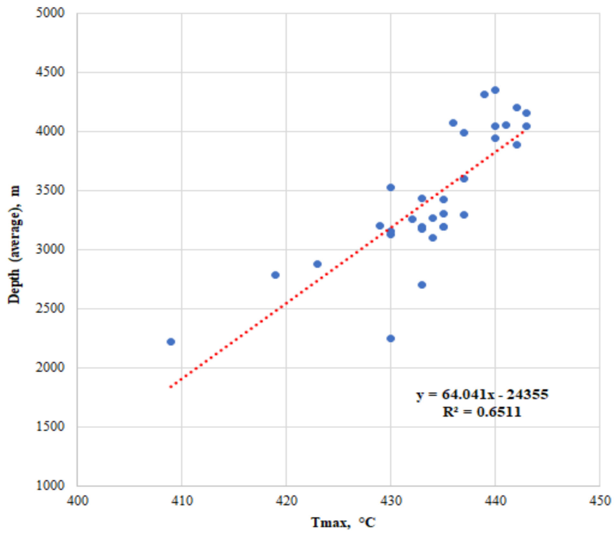

Figure 15. T_{max} (°C) variation vs. depth (m).

Considering the strong correlation between three parameters (S_1, S_2, TOC) and according to the linear models presented in Figure 16, a multiple linear regression model was assessed. The equation obtained is as follows:

$$TOC = 0.328 - 0.753 \times S_1 + 0.475 \times S_2 \quad (1)$$

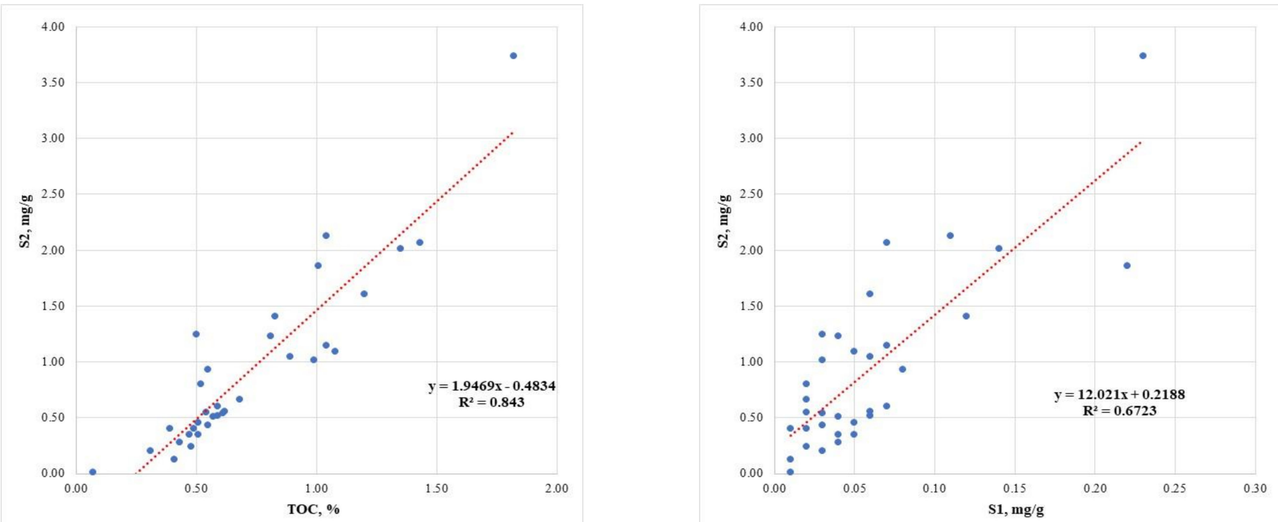

Figure 16. S_2 (mg HC/g rock) variation vs. TOC (wt%, **left**) and vs. S_1 (mg HC/g rock, **right**).

The model shows an extremely high adjusted R—square coefficient (R^2 = 0.846).

The model can be used for other values from the variation intervals of S_1 and S_2 variables for the estimation of TOC.

5. Conclusions

In the Getic Depression, the Upper Badenian organic matter is immature at depths between 2200–3200 m, with values of reflectance of 0.42%–0.49% and early mature at depths higher than 3200 m, with values of reflectance between 0.5%–0.55%. The types of organic matter are terrigenous and marine.

The type of terrigenous organic matter has a high diversity of macerals: vitrinite, liptinite (sporinite, resinite, cutinite) and inertinite. The marine organic matter has algae, as telalginite, lamalginite, and liptodetrinite, with *Tasmanites*, and *Leiosphaeridia* and other Prasinophyceae, in the following wells: A-1 Budieni, A-1 Rădinești, C-1,2 Socu, D-1, 3 Socu, B-1 Hurezani, B-1, 2 Bulbuceni, A-1 Logrești, A-1, 2, 3 Bibești, B-2, 3 Bibești, A-2 Piscu Stejarului. The Hydrogen Index of the Upper Badenian samples is less than 200 (mg HC/g TOC), as the shales contain gas prone, type III kerogen, in the frame of a C-type oganic facies.

Although pyrite occurrence alone is not enough for demonstrating the anoxic conditions, it is a useful marker to assess depositional conditions. Thus, pyrite occurs generally as framboidal and dispersed, associated with iron carbonates (siderite) in Vladimir-Totea, Rădinești, Bibești, Bulbuceni (showing anoxic conditions). In Colibași, Socu, Logrești, Piscu Stejarului, Drăganu, structures (showing oxic conditions), anoxic-oxic variable depositional conditions occur.

Most of samples with values of total organic carbon (TOC) < 1% wt.% have a limited potential of hydrocarbons (HC) generation, and 30% of samples with TOC < 1.82 wt.% and kerogen type III, present particularly gas generation potential. The samples have poor generation potential, depending on S_2 (mg HC/g rock) values, which are lower than 2.5 mg/g, only a single sample having S_2 value of 3.74 mg/g (A-1 Grădiște). The dominant kerogen is type III.

The statistical assessment highlighted the existence of some interesting relationships between the investigated parameters, among which the model between S_1, S_2, TOC can be used for other values from the variation intervals of these variables.

Author Contributions: Conceptualization, M.D.G.; methodology, M.D.G. and Ș.G.; software, M.D.G., Ș.G., N.M.B. and I.M., validation, M.D.G. and Ș.G.; formal analysis, M.D.G., Ș.G. and N.M.B.; investigation, M.D.G., M.E.P., G.P., Ș.G. and N.M.B.; data curation: M.D.G. and Ș.G.; writing—original draft preparation, M.D.G., M.E.P. and G.P.; writing—review and editing, M.D.G., M.E.P., G.P., I.M. and Ș.G.; visualization, M.D.G. and I.M., Ș.G.; supervision, M.E.P. and G.P. All authors have read and agreed to the published version of the manuscript.

Funding: This research received no external funding.

Data Availability Statement: OMV-PETROM S.A. I.C.P.T. Câmpina is the repository of the data supporting the results.

Acknowledgments: The authors gratefully acknowledge OMV-PETROM S.A. I.C.P.T. Câmpina company for allowing to publish geological, petrographical and geochemical data and results. The authors also acknowledge the constructive contributions of several anonymous peer-reviewers who improved the quality of the manuscript.

Conflicts of Interest: The authors declare no conflict of interest.

References

1. Ghiran, M.D.; Popa, M.E.; Mariș, I.; Gheorghe, S. Petrography and geochemistry of dispersed organic matter in the Oligocene source rocks of the central-western part of the Getic Depression, Romania. *Int. J. Coal Geol.* **2018**, *200*, 153–165. [CrossRef]
2. Paraschiv, D. Geology of hydrocarbon fields in Romania, Institute of Geology and Geophysics. *Tech. Econ. Stud. Ser. A* **1975**, *10*, 375. (In Romanian)
3. Paraschiv, D. *Romanian Oil and Gas Fields*; Institute of Geology and Geophysics: Bucharest, Romania, 1979; Volume 383. (In Romanian)
4. Motaş, C.; Nicolae, E.; Tudoran, C.; Horia, G.; Carp, V.; Giuglan, F.; Mihai, S.; Mihalache, M. *Reconstruction of the Geological Evolution of the Getic Depression for the Qualitative Evaluation of the Oil Potential and the Specification of the Optimal Hydrocarbon Storage Areas*; Geological Report: Petrom, SA, USA, 1995.
5. Popescu, B.M. Romania's petroleum systems and their remaining potential. *Pet. Geosci.* **1995**, *1*, 337–350. [CrossRef]
6. Buliga, G.; Balteş, N. Petroleum systems in the Getic fields: Folded internal foreland structures. *Oil Gas Monit.* **2006**, *5*, 51. (In Romanian)
7. Buliga, G.; Balteş, N. Petroleum Systems in the Getic Depression. *Oil Gas Monit.* **2006**, *5*, 22–24. (In Romanian)
8. Ştefănescu, M.; Dicea, O.; Butac, A.; Ciulavu, D. Hydrocarbon Geology of the Romanian Carpathians, their Foreland, and the Transylvanian Basin. *AAPG* **2006**, *84*, 521–567.

9. Krézsek, C.; Oterdoom, H.; Dzido, P.; Barbu, V.; Bland, S.; Amberger, K.; Lepădat, A. New Insights into The Hydrocarbon System of The Getic Depression, Romania: Implications for Exploration. In *73rd EAGE Conference & Exhibition Incorporating SPE EUROPEC*; Didactical and Pedagogical Publishing House: Bucharest, Romania, 2011.
10. Pawlewicz, M. Total Petroleum Systems of the Carpathian—Balkanian Basin Province of Romania and Bulgaria. *USGS* **2007**, *2204*, 17.
11. Băncilă, I. *Geology of the Eastern Carpathians*; Editura Tehnică: Bucharest, Romania, 1958; p. 368. (In Romanian)
12. Gavăt, I. *Petroleum Geology and Natural Gas*; Didactical and Pedagogical Publishing House: Bucharest, Romania, 1964; p. 303. (In Romanian)
13. Mocuța, S.T.; Past, Present, and Future of the Research-Development (R&D). Activity related to the Upstream Segment of Romania's Petroleum Industry. *Rev. Română De Pet. Ser. Nouă* **2009**, *16*, 5–12.
14. Mocuța, S.T. *Petroleum Basins and Fields on Earth*; Publishing House of the Romanian Academy: Bucharest, Romania, 2017; p. 81. (In Romanian)
15. Balteș, N. Metamorphism of different types of organic matter from sedimentary rocks of Romania and their importance for oil generation. In Proceedings of the 10th World Petroleum Congress, Bucharest, Romania, 9–14 September 1979; 43–47.
16. Balteș, N. *Complex Research Laboratory for the Knowledge of the Formation of Hydrocarbon Fields in the Northern Flank of the Getic Depression—Technical Report*; Arhiva OMV—Petrom SA: Bucharest, Romania, 1980. (In Romanian)
17. Balteș, N. Hydrocarbon source rocks in Romania. *Annu. De L'institut De Geol. Et De Geophys.* **1983**, *60*, 265–270.
18. Motaş, C. *New Data on Structural Relationships between the Southern Carpathians and the Getic Depression Lucr. Congr. XXI Assoc. Carp-Balc*; Institute of Geology and Geophysics: Bucharest, Romania, 1983; Volume 141–146. (In Romanian)
19. Buliga, G. Geological research for hydrocarbons in Greater Romania. *NOEMA* **2012**, *11*, 347–355. (In Romanian)
20. Krézsek, C. Petroleum Systems of Romania. *AAPG Eur. Reg.* **2011**, *10349*, 4–7.
21. Burgess, J.D. Microscopic Examination of Kerogen (Dispersed Organic Matter) in Petroleum Exploration. *Geol. Soc. Am. Spec. Pap.* **1974**, *153*, 19.
22. Espitalié, J.; Laporte, J.L.; Madec, M.; Marquis, F.; Leplat, P.; Paulet, J.; Boutefeu, A. Methode rapide de caracterisation des roches meres, de leur potential petrolier et de leur degree d'evolution. *Rev. Inst. Français Pet. Paris* **1997**, *32*, 23–42.
23. Durand, B. (Ed.) *Kerogen Insoluble Organic Matter from Sedimentary Rocks*; Institut Français du Pétrole: Paris, France, 1980; p. 474.
24. Behar, F.; Beaumont, V.; Penteado, H.L. de B. Rock-Eval technology: Performances and developments. *Oil Gas Sci. Technol.* **2001**, *56*, 111–134. [CrossRef]
25. Peters, K.E. Guidelines for evaluating petroleum source rock using programmed pyrolysis. *Am. Assoc. Pet. Geol. Bull.* **1986**, *70*, 318–329.
26. Espitalié, J.; Deroo, G.; Marquis, F. Rock Eval pyrolysis and its applications. *Inst. Français Du Pet. Paris* **1985**, *27299*, 79008.
27. Peters, K.E.; Cassa, M.R. Applied source rock geochemistry. In *The Petroleum System—From Source to Trap*; Magoon, L., Dow, W., Eds.; AAPG Memoir: Tulsa, OK, USA, 1994; pp. 93–120.
28. Bordenave, M.L. (Ed.) *Applied Petroleum Geochemistry*; Editions Technip: Paris, France, 1993; pp. 210–366.
29. Bordenave, M.L.; Espitalié, J.; Leplat, P.; Oudin, J.L.; Vandenbrouke, M. Screening techniques for source rock evaluation. *Appl. Petrol.* **1993**, *1993*, 217–278.
30. Hunt, J.M. *Petroleum Geochemistry and Geology*; Freeman and Company: San Francisco, CA, USA, 1995; p. 743.
31. Senftle, J.T.; Landis, C.R.; McLaughlin, R.L. Organic Petrographic Approach to Kerogen Characterization. In *Organic Geochemistry*; Springer: Boston, MA, USA, 1993; Volume 2239, pp. 355–374.
32. Hartkopf-Fröder, C.; Königshof, P.; Littke, R.; Schwarzbauer, J. Optical thermal maturity parameters and organic geochemical alteration at low grade diagenesis to anchimetamorphism: A review. *Int. J. Coal Geol.* **2015**, *150*, 74–119. [CrossRef]
33. Spina, A.; Vecoli, M.; Riboulleau, A.; Clayton, G.; Cirilli, S.; Di Michele, A.; Marcogiuseppe, A.; Rettori, R.; Sassi, P.; Servais, T.; et al. Application of Palynomorph Darkness Index (PDI) to assess the thermal maturity of palynomorphs: A case study from North Africa. *Int. J. Coal Geol.* **2018**, *188*, 64–78. [CrossRef]
34. Galasso, F.; Fernandes, P.; Montesi, G.; Marques, J.; Spina, A.; Pereira, Z. Thermal history and basin evolution of the Moatize—Minjova Coal Basin (N'Condédzi sub-basin, Mozambique) constrained by organic maturation levels. *J. Afr. Earth Sci.* **2019**, *153*, 219–238. [CrossRef]
35. Sorci, A.; Cirilli, S.; Clayton, G.; Corrado, S.; Hints, O.; Goodhue, R.; Schito, A.; Spina, A. Palynomorph optical analyses for thermal maturity assessment of Upper Ordovician (Katian-Hirnantian) rocks from Southern Estonia. *Mar. Pet. Geol.* **2020**, *120*, 104574. [CrossRef]
36. Spina, A.; Cirilli, S.; Sorci, A.; Schito, A.; Clayton, G.; Corrado, S.; Fernandes, P.; Galasso, F.; Montesi, G.; Pereira, Z.; et al. Assessing thermal maturity through a multi-proxy approach: A case study from the Permian Faraghan Formation (Zagros Basin, Southwest Iran). *Geosciences* **2021**, *11*, 484. [CrossRef]
37. Durand, B.; Alpern, B.; Pittion, J.L.; Pradier, B. Reflectance of vitrinite as a control of thermal history of sediments. In *Thermal Modelling in Sedimentary Basins*; Technip: Paris, France, 1986; pp. 441–474.
38. Tissot, B.P.; Welte, D.H. *Petroleum Formation and Occurrence*; Springer: Berlin, Germany, 1984; Volume 699.
39. Tissot, B.P.; Pellet, R.; Ungerer, P.H. Thermal history of sedimentary basins, maturation indices and kinetics of oil and gas generation. *AAPG Bull.* **1987**, *71*, 1445–1466.
40. Waples, D.W. *Geochemistry in Petroleum Exploration*; Resources and Develop. Co.: Boston, MA, USA, 1985; Volume 232.

41. Van Krevelen, D.W. *Coal, Typology, Chemistry, Physics, Constitution*; Elsevier: Amsterdam, The Netherlands, 1961; Volume 514.
42. Schito, A.; Corrado, S.; Trolese, M.; Aldega, L.; Caricchi, C.; Cirilli, S.; Grigo, D.; Guedes, A.; Romano, C.; Spina, A.; et al. Assessment of thermal evolution of Paleozoic successions of the Holy Cross Mountains (Poland). *Mar. Pet. Geol.* **2017**, *80*, 112–132. [CrossRef]
43. Schito, A.; Spina, A.; Corrado, S.; Cirilli, S.; Romano, C. Comparing optical and Raman spectroscopic investigations of phytoclasts and sporomorphs for thermal maturity assessment: The case study of Hettangian continental facies in the Holy cross Mts. (central Poland). *Mar. Pet. Geol.* **2019**, *104*, 331–345. [CrossRef]
44. Schito, A.; Atouabat, A.; Muirhead, D.K.; Calcagni, R.; Galimberti, R.; Romano, C.; Spina, A.; Corrado, S. An insight on the polyphase thermal history of the Internal Rif (Northern Morocco) through Raman micro-spectroscopy investigation. *Ital. J. Geosci.* **2022**, *141*, 104–119. [CrossRef]
45. Spina, A.; Brogi, A.; Capezzuoli, E.; Ventruti, G.; Zucchi, M.; Aldinucci, M.; Liotta, D. Use of palynology and thermal maturity in deformed geological units: A case study from the Permian succession in the Monte Leoni area (Middle Tuscan Ridge, inner Northern Apennines, Italy). *Sediment. Geol.* **2022**, *438*, 106210. [CrossRef]
46. Teichmüller, M. Organic petrology of source rocks, history and state of the art. *Org. Geochem.* **1986**, *10*, 581–599. [CrossRef]
47. Teichmüller, M.; Durand, B. Fluorescence microscopical rank studies on liptinites and vitrinites in peat and coals, and comparison with results of the Rock-Eval pyrolysis. *Int. J. Coal Geol.* **1983**, *2*, 197–230. [CrossRef]
48. Taylor, G.H.; Teichmüller, M.; Davis, A.; Diessel, C.F.K.; Littke, R.; Robert, P. *Organic Petrology*; Gebrüder Borntraeger: Stuttgart, Germany, 1998.
49. Staplin, F.L. (Ed.) Determination of thermal alteration index from color of exinite (pollen, spores). In *How to Assess Maturation and Paleotemperatures*; SEPM Short Course: Tulsa, OK, USA, 1982; pp. 7–11.
50. Stasiuk, L.D.; Fowler, M.G. Organic facies in Devonian and Mississippian strata of Western Canada sedimentary basin: Relation to kerogen type, paleoenvironment, and paleogeography. *Bull. Can. Petrol. Geol.* **2004**, *52*, 234–255. [CrossRef]
51. Kus, J.; Araujo, C.V.; Borrego, A.G.; Flores, D.; Hackley, P.C.; Hamor-Vido, M.; Kalaitzidis, S.; Kommeren, C.J.; Kwiecinska, B.; Mastalerz, M.; et al. Identification of alginite and bituminite in rocks other than coal. 2006, 2009, and 2011 round robin exercises of the ICCP Identification of Dispersed Organic Matter Working Group. *Int. J. Coal Geol.* **2017**, *178*, 26–38. [CrossRef]
52. Hackley, P.; Cardott, B.J. Application of organic petrography in North American shale petroleum systems: A review. *Int. J. Coal. Geol.* **2016**, *163*, 8–51. [CrossRef]
53. Panaitescu, C.; Penu, A. Microscopic characterization of organic and mineral matter in rock and kerogen samples. *IPB—Petromar* **1988**, *55*, 84–118. (In Romanian)
54. Panaitescu, C. Petrography of Coal, Coke and Carbonaceous Products. *Encycl. Publ. House* **1991**, *323*, 15146. (In Romanian)
55. Cardott, B.J.; Lambert, M.W. Thermal maturation by vitrinite reflectance of the Woodford shale, Anadarko Basin, Oklahoma. *AAPG Bull.* **1985**, *69*, 1982–1988.
56. Ghiran, M.D.; Popa, M.E.; Gheorghe, S. Characterization and evaluation of Badenian source rocks from the Central- Southern part of the Getic Depression, Romania. In Proceedings of the 71st Annual Meeting of the International Committee for Coal and Organic Petrology (ICCP), Symposium on Organic Petrology with special focus Oil Generation from Coals and Carbonaceous Shales, Hague, The Netherlands, 16–20 September 2019.
57. Ghiran, M.D.; Popa, M.E.; Gheorghe, Ș. *Identification of Macerals from Badenian Source Rocks of Centre Part of the Getic Depression*; Geodoct Symposium: Bucharest, Romania, 2020.
58. Săndulescu, M. *Geotectonics of Romania*; Technical Publishing House: Bucharest, Romania, 1984; p. 335. (In Romanian)
59. Mutihac, V. *The Geological Structure of Romania*; Technical Publishing House: Bucharest, Romania, 1990; p. 419. (In Romanian)
60. Mutihac, V.; Stratulat, M.I.; Fechet, R.M. *Geology of Romania*; Didactic and Pedagogical Publishing House: Bucharest, Romania, 2004; p. 249. (In Romanian)
61. Mațenco, L.; Bertotti, G.; Dinu, C.; Cloetingh, S. Tertiary tectonic evolution of the external South Carpathians and the adjiacent Moesian platform (Romania). *Tectonics* **1997**, *16*, 896–911. [CrossRef]
62. Răbăgia, T.; Füllop, A. Syntectonic sedimentation history in the Southern Carpathians foredeep, Berza, T., ALCAPA II: Geological evolution of the Alps-Carpathian-Pannonian System, Abstracts volume. *Rom. J. Tecton. Regn. Geol.* **1994**, *75*, 48.
63. Mațenco, L.; Schmid, S.M. Exhumation of the Danubian nappe system (South Carpathians) during the Early Tertiary: Inferences from kinematic and paleostress analysis at the Getic/Danubian nappe contact. *Tectonophysics* **1999**, *314*, 401–422. [CrossRef]
64. Mațenco, L.; Bertotti, G. Tertiary tectonic evolution of the external East Carpathians (Romania). *Tectonophysics* **2000**, *316*, 255–286. [CrossRef]
65. Mațenco, L.; Krézsek, C.; Merten, S.; Schmid, S.M.; Cloetingh, S.; Andriessen, P. Characters of collisional orogens with low topographic build-up: An example from the Carpathians. *Terra Nova* **2010**, *22*, 155–165. [CrossRef]
66. Schmid, S.M.; Bernoulli, D.; Fugenschuh, B.; Mațenco, L.; Schefer, S.; Schster, R.; Tischler, M.; Ustaszewski, K. The Alpin-Carpathian-Dinaridic orogenic system Correlation and evolution of tectonic units. *Swiss J. Geosci.* **2008**, *101*, 139–183. [CrossRef]
67. Răbăgia, T.; Maţenco, L. Tertiary tectonic and sedimentological evolution of the South Carpathians foredeep: Tectonic versus eustatic control. *Mar. Pet. Geol.* **1999**, *16*, 719–740. [CrossRef]
68. Kräutner, H.C.; Krstić, B. Alpine and Pre-Alpine structural units within the Southern Carpathians and the Eastern Balkanides. *Proc. XVII. Congr. Carpathian-Balk. Geol. Assoc. Bratisl. Geol. Carpathica Spec. Issue* **2002**, *53*, 7.

69. Bădescu, D. *The Tectono-Stratigraphic Evolution of the Eastern Carpathians during the Mesozoic and Neozoic*; Economic Publishing House: Bucharest, Romania, 2005; Volume 312. (In Romanian)
70. Tărăpoancă, M.; Ţambrea, D.; Avram, V.; Popescu, B. The geometry of the south leading Carpathian thrust line and the Moesia boundary: The role of inherited structures in establishing a transcurrent contact on the concave side of the Carpathians. In *Thrust Belts and Foreland Basins: From Fold Kinematics to Hydrocarbon Systems: Frontiers in Earth Sciences*; Lacombe, O., Lave, J., Roure, F., Verges, J., Eds.; Springer: Berlin/Heidelberg, Germany, 2007; pp. 492–508.
71. Krézsek, C.; Lăpădat, A.; Mațenco, L.; Arnberger, K.; Barbu, V.; Olaru, R. Strain partitioning at orogenic contacts during rotation, strike-slip and oblique convergence: Palaeogene-Early Miocene evolution of the contact between the South Carpathians and Moesia. *Glob. Planet. Chang.* **2013**, *103*, 63–81. [CrossRef]
72. Răbăgia, T.; Roban, R.D.; Tărăpoancă, M. Sedimentary records of Palaeogene (Eocene to Lowermost Miocene) deformations near the contact between the Carpathian Thrust Belt and Moesia. *Oil and Gas Sci. Technol.* **2011**, *66*, 931–952. [CrossRef]
73. *SR ISO 5069-2: 1994*; Brown Coals and Lignites. Principles of Sampling. Part 2: Sampling for Determination of Moisture Content and for General Analysis. Romanian Standard Association: Bucharest, Romania, 1994; Volume 14.
74. *ISO 7404-2:2009*; Methods for the Petrographic Analysis of Coals-Part 2: Methods of Preparing Coal Samples. International Organization for Standardization: Geneva, Switzerland, 2009; p. 12.
75. *ASTM D7708-11*; Standard Test Method for Microscopical Determination of the Reflectance of Vitrinite Dispersed in Sedimentary Rocks. Annual Book of ASTM Standards: Petroleum Products, Lubricants, and Fossil Fuels; Gaseous Fuels; Coal and Coke. ASTM International: West Conshohocken, PA, USA, 2014.
76. Lafarque, E.; Marquis, F.; Pilot, D. Rock-Eval 6 applications in hydrocarbon exploration; production, and soil contamination studies. *Rev. De L'institut Français Du Pet.* **1998**, *53*, 421–437. [CrossRef]
77. ICCP. The new vitrinite classification (ICCP System 1994). *Fuel* **1998**, *77*, 349–358. [CrossRef]
78. Pickel, W.; Kus, J.; Flores, D.; Kalaitzidis, S.; Christanis, K.; Cardott, B.J.; Misz-Kennan, M.; Rodrigues, S.; Hentschel, A.; Hamor-Vido, M.; et al. Classification of liptinite-ICCP System 1994. *Int. J. Coal Geol.* **2017**, *169*, 40–61. [CrossRef]
79. Sýkorová, I.; Pickel, W.; Christanis, K.; Wolf, M.; Taylor, G.H.; Flores, D. Classification of huminite- ICCP System 1994. *Int. J. Coal Geol.* **2005**, *62*, 85–106. [CrossRef]
80. ICCP. The new inertinite classification (ICCP System 1994). *Fuel* **2001**, *80*, 459–471. [CrossRef]
81. Panaitescu, C.; Predeanu, G. *Carbopetrographic Atlas*; Publishing House of the Romanian Academy: Bucharest, Romania, 1999; Volume 264. (In Romanian)
82. Falcon, R.M.S.; Snyman, C.P. An introduction to coal petrography: Atlas of petrographic constituents in the bituminous coals of Southern Africa. *Geol. Soc. South Afr.* **1986**, *2*, 106.
83. Wagner, N.; Malumbazo, N.; Falcon, R. *Southern African Coals and Carbons*; Struik Nature: Cape Town, South Africa, 2018; p. 248.
84. Carr, A.D. Suppression and retardation of vitrinite reflectance, part 1. Formation and significance for hydrocarbon generation. *J. Pet. Geol.* **2000**, *23*, 313–343. [CrossRef]
85. Snowdon, L.R.; Fowler, M.G. Interpretation of organic geochemical data. In *Canadian Society of Petroleum Geologists*; Short Course Notes: Nutley, NJ, USA, 1997; Volume 86.